Wnt signaling promotes tumor development in part through phosphofructokinase 1 platelet isoform upregulation

SO MI JEON[1], JE SUN LIM[1], SU HWAN PARK[1] and JONG-HO LEE[1,2]

[1]Department of Health Sciences, The Graduate School of Dong-A University; [2]Department of Biological Sciences, Dong-A University, Busan 49315, Republic of Korea

Received January 4, 2021; Accepted July 21, 2021

DOI: 10.3892/or.2021.8185

Abstract. The activation of Wnt signaling has been detected in various types of human cancer and has been shown to be associated with cancer development. In the present study, it was revealed that Wnt signaling induced the expression of phosphofructokinase 1 platelet isoform (PFKP), which has been reported to catalyze a rate-limiting reaction in glycolysis and is important for the Warburg effect, proliferation, colony formation and cancer cell migration. Moreover, it was demonstrated that Wnt3A induced PFKP expression in a β-catenin-independent manner, resulting in increased PFK enzyme activity. Wnt3A-induced epidermal growth factor receptor transactivation activated PI3K/AKT, which stabilized PFKP through PFKP S386 phosphorylation and subsequent PFKP upregulation. Wnt3A-induced PFKP S386 phosphorylation increased PFKP expression and promoted the Warburg effect, cell proliferation, colony formation and the migratory ability of cancer cells. On the whole, the findings of the present study underscore the potential role of PFKP in Wnt signaling-induced tumor development.

Introduction

Wnt signaling is implicated in various physiological processes, including cell proliferation and differentiation, metabolism, development, tissue homeostasis and tissue regeneration (1-6). In addition, the aberrant activation of Wnt signaling, which contributes to cancer progression, invasion, metastasis and recurrence, has been detected in various types of cancer, including epidermoid, breast, prostate and lung malignancies, as well as in glioblastoma (GBM) (7-9). Notably, Wnt3A has been reported to be overexpressed in the human tumor microenvironment and in tumor cells (10-13). Additionally, Wnt3A expression has been reported to be associated with tumor grade (12,13). Wnt3A is considered to function as an oncogenic factor through the promotion of proliferation, invasion, metastasis and chemo/radioresistance in a number of tumor types, including epidermoid, breast, prostate and hepatocellular malignancies, as well as in GBM (12-16).

In general, Wnt signaling is classified into the canonical Wnt pathway (β-catenin-dependent) and the non-canonical Wnt pathway (β-catenin-independent) (17,18). In the canonical Wnt pathway, the binding of Wnt ligand to the low-density lipoprotein receptor-related protein-5/6 and Frizzled receptors results in the inhibition of the GSK-3β-mediated phosphorylation of β-catenin. Subsequently, this promotes β-catenin stabilization and translocation to the nucleus, where β-catenin interacts with T-cell-specific factor (TCF)/lymphoid enhancer-binding factor (LEF) and coactivators, in order to activate Wnt target genes involved in the development of cancer (19-23). In the non-canonical Wnt pathway, Wnt signaling activates phospholipase C or small GTPases through the binding of the Wnt ligand to Frizzled receptors and Ror/Ryk co-receptors or Frizzled receptors, respectively, inducing a wide range of cellular processes, including actin cytoskeleton remodeling and cell motility (8,22,24). Accumulating evidence has indicated that cancer cells acquire the ability to migrate and metastasize through the non-canonical Wnt pathway (7,24-26).

The Warburg effect, a key metabolic hallmark of cancer, is the phenomenon through which cancer cells produce energy, predominantly through aerobic glycolysis and regardless of the extracellular oxygen levels (27). Due to the reduced efficiency of glycolysis in ATP production, cancer cells increase glucose uptake for ATP production, followed by lactic acid fermentation in the cytosol (28). This metabolic alteration is required for the increased energy and biosynthetic demands of tumor cells and facilitates their rapid growth (29,30). β-catenin-dependent canonical Wnt signaling has been found to be indirectly involved in the regulation of glycolysis though the regulation of mitochondrial enzyme expression, including pyruvate dehydrogenase kinase 1 and pyruvate carboxylase (31,32). However, whether the β-catenin-independent non-canonical Wnt signaling directly regulates the Warburg effect in cancer cells remains unknown.

In glucose metabolism, phosphofructokinase 1 (PFK1), which catalyzes the rate-limiting reaction of glycolysis,

Correspondence to: Professor Jong-Ho Lee, Department of Health Sciences, The Graduate School of Dong-A University, 37 Nakdong-Daero 550 beon-gil, Saha-gu, Busan 49315, Republic of Korea
E-mail: topljh19@dau.ac.kr

Key words: Wnt, epidermal growth factor receptor, transactivation, AKT, phosphofructokinase 1 platelet isoform, phosphorylation

converts fructose 6-phosphate and ATP to fructose 1,6-bisphosphate and ADP (33). PFK1 has three isoforms, PFK1 platelet (PFKP), PFK1 liver (PFKL) and PFK1 muscle (PFKM), as originally named, since PFKL is the most abundant isoform in the liver, whereas PFKM and PFKP are the only isoforms present in muscles and platelets in adults, respectively (33,34). However, all three isoforms have been detected in the brain and other tissues (35,36). Additionally, it has been previously reported by the authors that all three isoforms are expressed in GBM cells; PFKP is the prominent PFK1 isoform in GBM cells and has been found to be overexpressed in human GBM specimens (37). AKT-mediated phosphorylation of PFKP at S386 inhibits the proteasomal degradation of PFKP, resulting in the increased PFKP expression and promoting aerobic glycolysis and brain tumor growth (37). However, the role of PFKP in Wnt signaling-induced tumor development remains unknown.

In the present study, it was demonstrated that Wnt signaling transactivated epidermal growth factor receptor (EGFR) in order to induce PI3K/AKT activation, resulting in PFKP phosphorylation at S386 and stabilizing PFKP protein, thereby promoting the Warburg effect, as well as cell proliferation, colony formation and cancer cell migration.

Materials and methods

Reagents and antibodies. The following reagents and antibodies were purchased from the indicated companies: Rabbit polyclonal antibodies recognizing PFKP (cat. no. 12746, 1:1,000 for western blot analysis), phosphorylated (p-)AKT (pT308, cat. no. 4056, 1:1,000 for western blot analysis), p-AKT (pS473, cat. no. 4060, 1:1,000 for western blot analysis) and AKT (cat. no. 9272, 1:1,000 for western blot analysis) from Cell Signaling Technology, Inc.; mouse monoclonal antibodies for PFKL (A-6, cat. no. sc-393713, 1:500 for western blot analysis), PFKM (cat. no. sc-67028, 1:1,000 for western blot analysis), PFK2 (cat. no. sc-377416, 1:500 for western blot analysis), lactate dehydrogenase A (LDHA) (cat. no. sc-137243, 1:500 for western blot analysis) and β-catenin (E-5, cat. no. sc-7963, 1:200 for western blot analysis) from Santa Cruz Biotechnology, Inc.; mouse monoclonal antibody for tubulin (clone B-5-1-2, T6074, 1:5,000 for western blot analysis) from MilliporeSigma; rabbit polyclonal antibodies for EGFR (pY869, cat. no. 11229, 1:1,000 for western blot analysis) and PFKP [pS386, 1:1,000 for western blot analysis; customized as previously described (37)] from Signalway Antibody LLC; mouse monoclonal EGFR antibody (cat. no. 610016, 1:1,000 for western blot analysis) from Abcam; human recombinant EGF (E9644) and cycloheximide (CHX; 66-81-9) from MilliporeSigma; Wnt3A (5036-WN) from R&D Systems, Inc.; AG1478 (658552) from Calbiotech, Inc.; LY294002 (L-7988) from LC Laboratories; MK-2206 (S1078) from Selleck Chemicals; DAPI and Alexa Fluor 488 goat anti-rabbit antibody (A11008, 1:10,000 for immunofluorescence) from Molecular Probes; Thermo Fisher Scientific, Inc.; HyFect transfection reagents (E2650) from Denville Scientific, Inc.

Cell culture. A431 (21555) human epidermoid carcinoma cells and MDA-MB-231 (30026) human breast carcinoma cells were purchased from the Korean Cell Line Bank (KCLB). LN18 and LN229 GBM cells were kindly provided by Dr Hyunggee Kim (Korea University, Seoul, Korea). U251 GBM cells were kindly provided by Dr Kyu Heo (Dongnam Institute of Radiological and Medical Sciences, Busan, Korea). The human epidermal squamous carcinoma cell lines, SCC12 and SCC13, were kindly provided by Dr Tae-Jin Yoon (Gyeongsang National University and Hospital, Jinju, Korea). These cells were maintained in Dulbecco's modified Eagle's medium (DMEM), supplemented with 10% bovine calf serum (Capricorn Scientific GmbH) and 1% penicillin/streptomycin (Capricorn Scientific GmbH).

DNA constructs, mutagenesis, and transfection. PCR-amplified human PFKP was cloned into the pcDNA3.1/hygro(+)-Flag vector. pcDNA3.1/hygro(+)-Flag PFKP S386A was created using the QuikChange site-directed mutagenesis kit (Stratagene; Agilent Technologies, Inc.). The pGIPZ shRNA vector (RHS4348) was purchased from GE Dharmacon, Inc. shRNA-resistant (r) PFKP contained the a448c, g450c, c453t and c456g mutations. The following pGIPZ shRNAs were used: Control shRNA oligonucleotide, 5'-GCTTCTAACACCGGAGGTCTT-3'; PFKP shRNA oligonucleotide, 5'-AGGAACGGCCAGATCGATA-3'; and β-catenin shRNA oligonucleotide, 5'-TTACCACTCAGA GAAGGAG-3'. Cells were plated at a density of $4x10^5$/60-mm dish 18 h prior to transfection and were directly transfected with the constructed vectors (1 μg/6-well plate) using HyFect transfection reagent (Denville Scientific, Inc.) according to the manufacturer's instructions. Transfected cells were stabilized for 1 day, and then the cells were selected for 1 week using 200 μg/ml hygromycin (400053; EMD Millipore) and 2 μg/ml puromycin (540222; EMD Millipore).

Reverse transcription-quantitative PCR (RT-qPCR). Total RNA was prepared from tumor cells using an RNeasy Mini kit (Qiagen, Inc.) according to the manufacturer's instructions, and cDNA was synthesized from 2 μg of total RNA by reverse transcriptase (Superscript II Preamplification System, Gibco; Thermo Fisher Scientific, Inc.). Quantitative PCR (qPCR) was performed on an ABI Prism 7500 sequence detection system using a SYBR®-Green PCR Master Mix (Applied Biosystems; Thermo Fisher Scientific, Inc.) and following the manufacturer's protocols. The ABI 7500 sequence detector was programmed with the following PCR conditions: 40 cycles of 15-sec denaturation at 95˚C and 1-min amplification at 60˚C. All reactions were run in triplicate and normalized to the housekeeping gene β-actin. The evaluation of relative differences of PCR results was calculated using the $2^{-\Delta\Delta Cq}$ method (38). The following primer pairs were used for RT-qPCR: Human PFKP forward, 5'-CGGAAGTTCCTG GAGCACCTCTC-3' and reverse, 5'-AAGTACACCTTGGCC CCCACGTA-3'; human PFKL forward, 5'-GGCATTTAT GTGGGTGCCAAAGTC-3' and reverse, 5'-CAGTTGGCC TGCTTGATGTTCTCA-3'; human PFKM forward, 5'-GAG TGACTTGTTGAGTGACCTCCAGAAA-3' and reverse, 5'-CACAATGTTCAGGTAGCTGGACTTCG-3'; human PFKPB1 forward, 5'-AGAAGGGGCTCATCCATACCC-3' and reverse, 5'-CTCTCGTCGATACTGGCCTAA-3'; human PFKFB2 forward, 5'-AGTCCTACGACTTCTTTCGGC-3' and reverse, 5'-TCTCCTCAGTGAGATACGCCT-3'; human

PFKFB3 forward, 5'-ATTGCGGTTTTCGATGCCAC-3' and reverse, 5'-GCCACAACTGTAGGGTCGT-3'; human PFKFB4 forward, 5'-CAACATCGTGCAAGTGAAACT G-3' and reverse, 5'-GACTCGTAGGAGTTCTCATAGCA-3'; and human β-actin forward, 5'-ATGGATGATGATATCGCC GCGC-3' and reverse, 5'-GCAGCACGGGGTGCTCCTCG-3'.

Western blot analysis. Protein extraction from the cultured cancer cells was performed using a lysis buffer [50 mM Tris-HCl (pH 7.5), 0.1% SDS, 1% Triton X-100, 150 mM NaCl, 1 mM DTT, 0.5 mM EDTA, 100 μM sodium orthovanadate, 100 μM sodium pyrophosphate, 1 mM sodium fluoride, and proteinase inhibitor cocktail]. The cell extracts were centrifuged at 12,000 x g (at 4˚C for 15 min) and protein concentrations of cell lysates were determined using the DC protein assay kit (5000116, Bio-Rad Laboratories, Inc.). Equal amounts of lysates (2 mg/ml protein) were resolved by 8-10% SDS-PAGE and were then transferred to a nitrocellulose membrane. The membrane was blocked with 5% skim milk in TBST at room temperature for 1 h and then incubated with the indicated antibodies (as indicated above in Reagents and antibodies) at 4˚C overnight. The blots were then incubated with horseradish peroxidase-conjugated secondary antibodies (anti-rabbit (NA934V; Cytiva) or anti-mouse (NA931V; Cytiva) at a dilution of 1:3,000) at room temperature for 2 h and were visualized using a chemiluminescence technique (Amersham Biosciences). Band intensity was quantified using ImageJ 1.53e software (National Institutes of Health). Each experiment was repeated at least three times.

Immunofluorescence analysis. A431 cells were fixed with 4% paraformaldehyde for 20 min and permeabilized using 0.5% Triton X-100 at room temperature for 10 min. The cells were blocked with 5% normal serum at 37˚C for 30 min and incubated with an anti-PFKP antibody at a dilution of 1:100 at 4˚C overnight, subsequently, an Alexa Fluor dye-conjugated secondary antibody at 37˚C for 1 h, and in the end, stained with DAPI at room temperature for 10 min. The cells were examined using a deconvolution microscope (Zeiss AG) with a 63-Å oil-immersion objective. Axio Vision software from Zeiss AG was used to deconvolute the Z-series images.

Measurement of glucose consumption and lactate production. The A431 cells were seeded in culture dishes, and the medium was changed after 6 h with non-serum DMEM. The cells were then incubated at 37˚C for 48 h, and the culture medium was collected for the measurement of glucose and lactate concentrations. Glucose levels were determined using a glucose (GO) assay kit (GAGP20, Sigma-Aldrich; Merck KGaA). Glucose consumption was calculated as the difference in glucose concentration between the collected culture medium and DMEM. The absorbance was recorded at 540 nm at room temperature in a 96-well plate. Lactate levels were determined using a lactate assay kit (1200051002, Eton Bioscience, Inc.). The absorbance was recorded at 570 nm using a microplate reader (SpectraMax® ABS; Molecular Devices, LLC) at room temperature in a 96-well plate. All results were normalized to the final cell number.

Cell proliferation assay. A total of $2x10^4$ A431 cells were plated and incubated for 5 days after seeding in DMEM with 0.5% bovine calf serum. The cells were trypsinized and counted using a hemocytometer following staining with trypan blue at room temperature for 1 min (EBT-001; NanoEnTek, Inc.). The data represent the mean ± SD of three independent experiments.

Measurement of PFK activity. PFK activity was assessed in A431 cells with the use of the PFK activity colorimetric assay kit (K776-100, BioVision, Inc.). The reaction was performed using cell lysate (3 μg) in 100 μl of reaction buffer, which was prepared according to the instructions provided with the kit. The absorbance was recorded at 450 nm using a microplate reader (SpectraMax® ABS) at 37˚C in a 96-well plate.

Measurement of LDH activity. LDH activity was assessed in A431 cells using a lactate dehydrogenase activity colorimetric assay kit (K726-500, BioVision, Inc.). The reaction was performed using cell lysate (1 μg) in 100 μl of reaction buffer, which was prepared according to the instructions provided with the kit. The absorbance was recorded at 450 nm using a microplate reader (SpectraMax® ABS) at 37˚C in a 96-well plate.

Wound healing assay. A431 cells ($1.5x10^5$ cells/well) were seeded into 12-well plates and cultured at 100% confluence, followed by starvation in serum-free DMEM for 24 h. A sterile 200 μl pipette tip was used to create a scratch in the monolayer in the middle of the well. At the 0 and 18-h incubation at 37˚C time points, cells were photographed using a light microscope (x200 magnification) and the migration distance was measured using ImageJ 1.53e software (National Institutes of Health). The data represent the mean ± SD of three independent experiments.

Colony formation assay. A431 cells ($1x10^3$ cells/well) were seeded into 6-well plates and cultured in DMEM supplemented with 10% bovine calf serum with or without Wnt3A (20 ng/ml). Colony formation assay was performed for 7 or 12 days. The cells were fixed with 10% formalin (F8775, Sigma-Aldrich; Merck KGaA) for 10 min and stained with 0.1% crystal violet (V5265, Sigma-Aldrich) at room temperature for 1 h. The residual dye was washed off with water and the plate was air-dried.

Statistical analysis. All quantitative data are presented as the mean ± SD of at least three independent experiments. A 2-group comparison was conducted using the 2-sided, 2-sample Student's t-test. A simultaneous comparison of >2 groups was conducted using one-way ANOVA followed by Tukey's post hoc tests. The SPSS statistical package (version 12; SPSS Inc.) was used for the analyses. Values of $P<0.05$ were considered to indicate statistically significant differences.

Results

EGFR transactivation is required for the Wnt3A-induced the Warburg effect, as well as cell proliferation, colony formation and cancer cell migration. Wnt3A was used to stimulate A431, SCC12, and SCC13 human epidermal carcinoma cells, U251, LN229 and LN18 human GBM cells, and MDA-MB-231

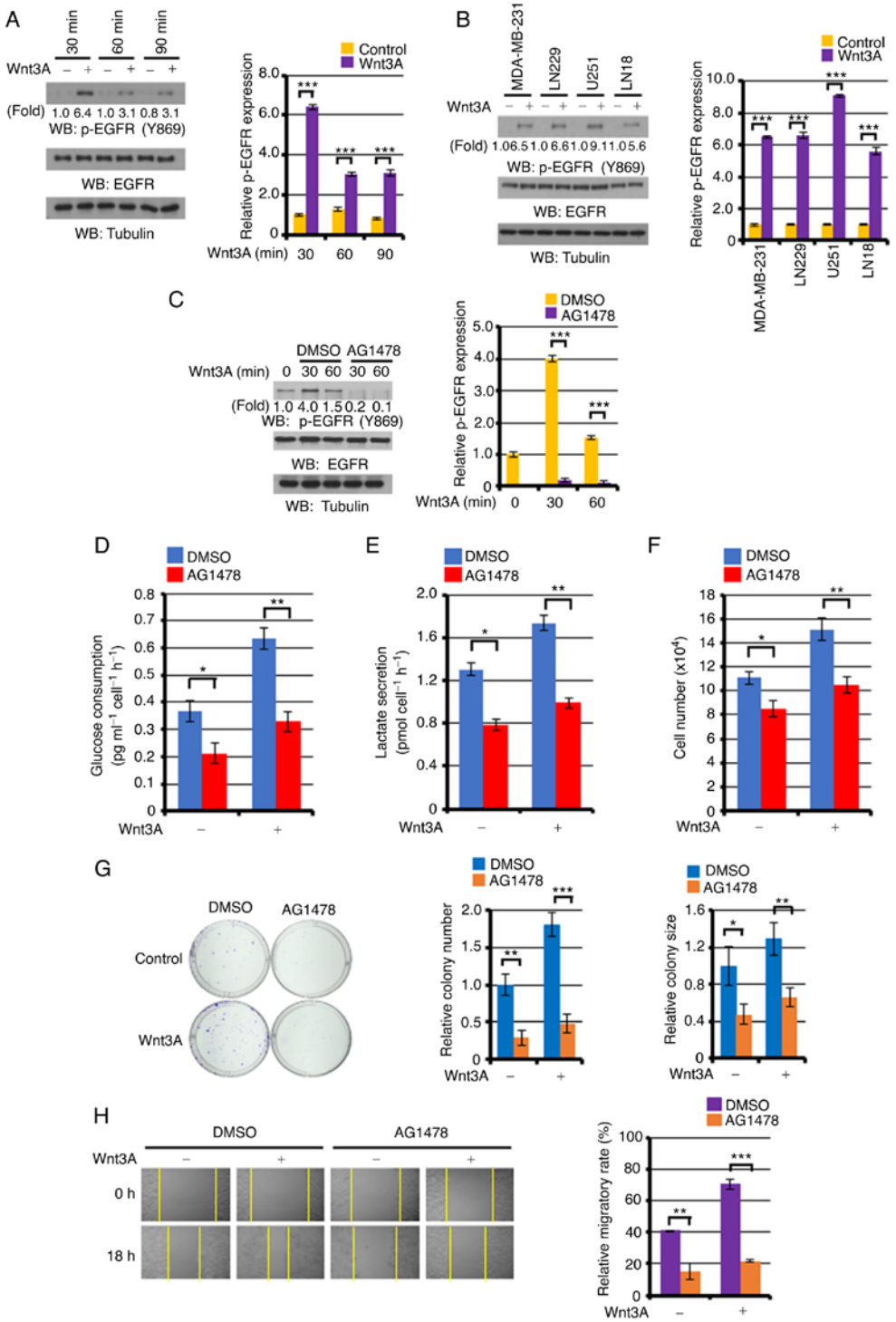

Figure 1. Effect of Wnt3A-induced EGFR transactivation on the Warburg effect, and the proliferation and migration of cancer cells. (A) Serum-starved A431 cells were stimulated with or without Wnt3A (20 ng/ml) for the indicated periods of time. Western blot analyses were performed with the indicated antibodies. Representative band intensity was quantified using ImageJ software. (B) Serum-starved MDA-MB-231, LN229, U251 and LN18 cells were stimulated with or without Wnt3A (20 ng/ml) for 30 min. Western blot analyses were performed with the indicated antibodies. Representative band intensity was quantified using ImageJ software. (C) Serum-starved A431 cells were stimulated with or without Wnt3A (20 ng/ml) for the indicated periods of time in the presence of DMSO or AG1478 (1 μM). Western blot analyses were performed with the indicated antibodies. Representative band intensity was quantified using ImageJ software. ***P<0.001 based on the Student's t-test. (D and E) A431 cells were cultured in serum-free DMEM with or without Wnt3A (20 ng/ml) for 48 h in the presence of DMSO or AG1478 (1 μM). The media were collected to analyze (D) glucose consumption and (E) lactate secretion. All results were normalized to cell number. The data represent the mean ± SD of three independent experiments. *P<0.05 and **P<0.01 based on the Student's t-test. (F) A431 cells were cultured in medium containing 0.5% serum with or without Wnt3A (20 ng/ml) for 96 h in the presence of DMSO or AG1478 (1 μM) and harvested for cell counting. The data represent the mean ± SD of three independent experiments. *P<0.05 and **P<0.01 based on the Student's t-test. (G) A431 cells were cultured in medium containing 10% serum with or without Wnt3A (20 ng/ml) for 7 days in the presence of DMSO or AG1478 (1 μM). The colonies were fixed with 10% formalin and stained with 0.1% crystal violet. Representative images are shown (left panel). Colony number (middle panel) and size (right panel) were analyzed. The data represent the mean ± SD of three independent experiments. *P<0.05, **P<0.01 and ***P<0.001 based on the Student's t-test. (H) Migration ability of A431 cells treated with or without Wnt3A (20 ng/ml) for 18 h in the presence of DMSO or AG1478 (1 μM) was assessed by wound healing assay. Representative images are shown (left panel). The quantification of migration ability is shown (right panel). The data represent the mean ± SD of three independent experiments. **P<0.01 and ***P<0.001 based on the Student's t-test.

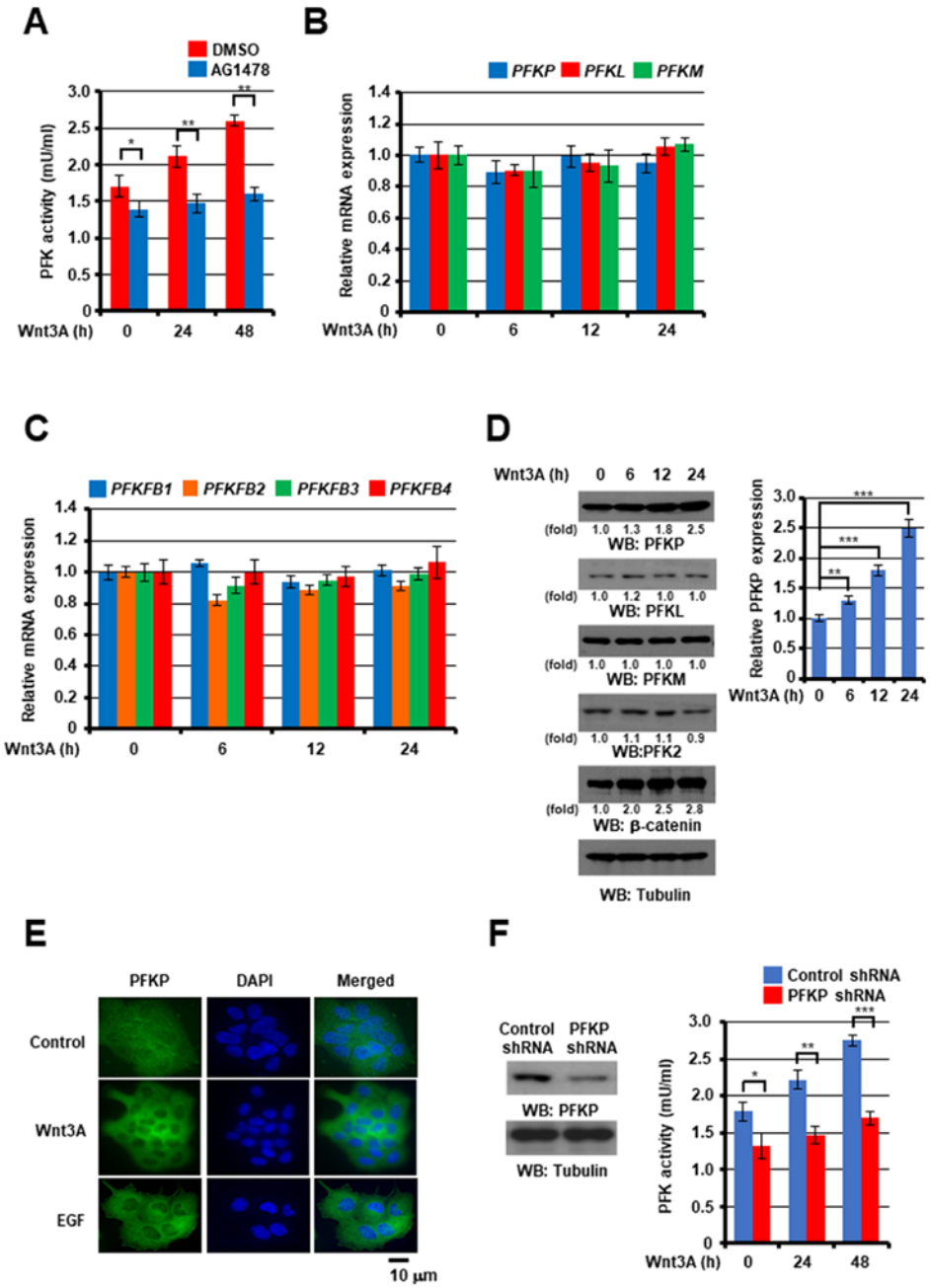

Figure 2. Effect of Wnt3A PFK enzyme activity and PFKP expression. (A) Serum-starved A431 cells were stimulated with or without Wnt3A (20 ng/ml) for the indicated periods of time in the presence of DMSO or AG1478 (1 μM). PFK enzymatic activity was measured. The data represent the mean ± SD of three independent experiments. *P<0.05 and **P<0.01 based on the Student's t-test. (B) Serum-starved A431 cells were stimulated with or without Wnt3A (20 ng/ml) for the indicated periods of time. The relative mRNA expression levels of PFK1 isoforms were determined. The data represent the mean ± SD of three independent experiments. (C) Serum-starved A431 cells were stimulated with or without Wnt3A (20 ng/ml) for the indicated periods of time. The relative mRNA expression levels of PFK2 isoforms were determined. The data represent the mean ± SD of three independent experiments. (D) Serum-starved A431 cells were stimulated with or without Wnt3A (20 ng/ml) for the indicated periods of time. Western blot analyses were performed with the indicated antibodies. Representative band intensity was quantified using ImageJ software. **P<0.01 and ***P<0.001 based on one-way ANOVA with Tukey's post hoc test. (E) Serum-starved A431 cells were stimulated with or without Wnt3A (20 ng/ml) or EGF (100 ng/ml) for 24 h and immunostained with an anti-PFKP antibody (scale bar, 10 μm). (F) A431 cells were transfected with PFKP shRNA or control shRNA. A431 cells stably expressing PFKP shRNA or control shRNA were used to analyze PFK enzymatic activity. The data represent the mean ± SD of three independent experiments. *P<0.05, **P<0.01 and ***P<0.001 based on the Student's t-test. PFK, phosphofructokinase 1; PFKP, phosphofructokinase 1 platelet isoform.

human breast carcinoma cells, in order to determine whether the Wnt-induced EGFR transactivation has effects on tumor development or not. As presented in Fig. 1A, Wnt3A stimulation significantly induced EGFR phosphorylation levels at 30, 60 and 90 min, as compared with the unstimulated control A431 cell EGFR levels. Similar results were also observed in other types of cancer cells: MDA-MB-231, LN229, U251 and LN18 (Fig. 1B), and SCC12 and SCC13 (Fig. S1). Pre-treatment with the specific EGFR tyrosine kinase inhibitor, AG1478, following the successful blocking of Wnt3A-induced EGFR phosphorylation (Fig. 1C), markedly abrogated both basal and Wnt3A-enhanced glucose consumption (Fig. 1D), lactate

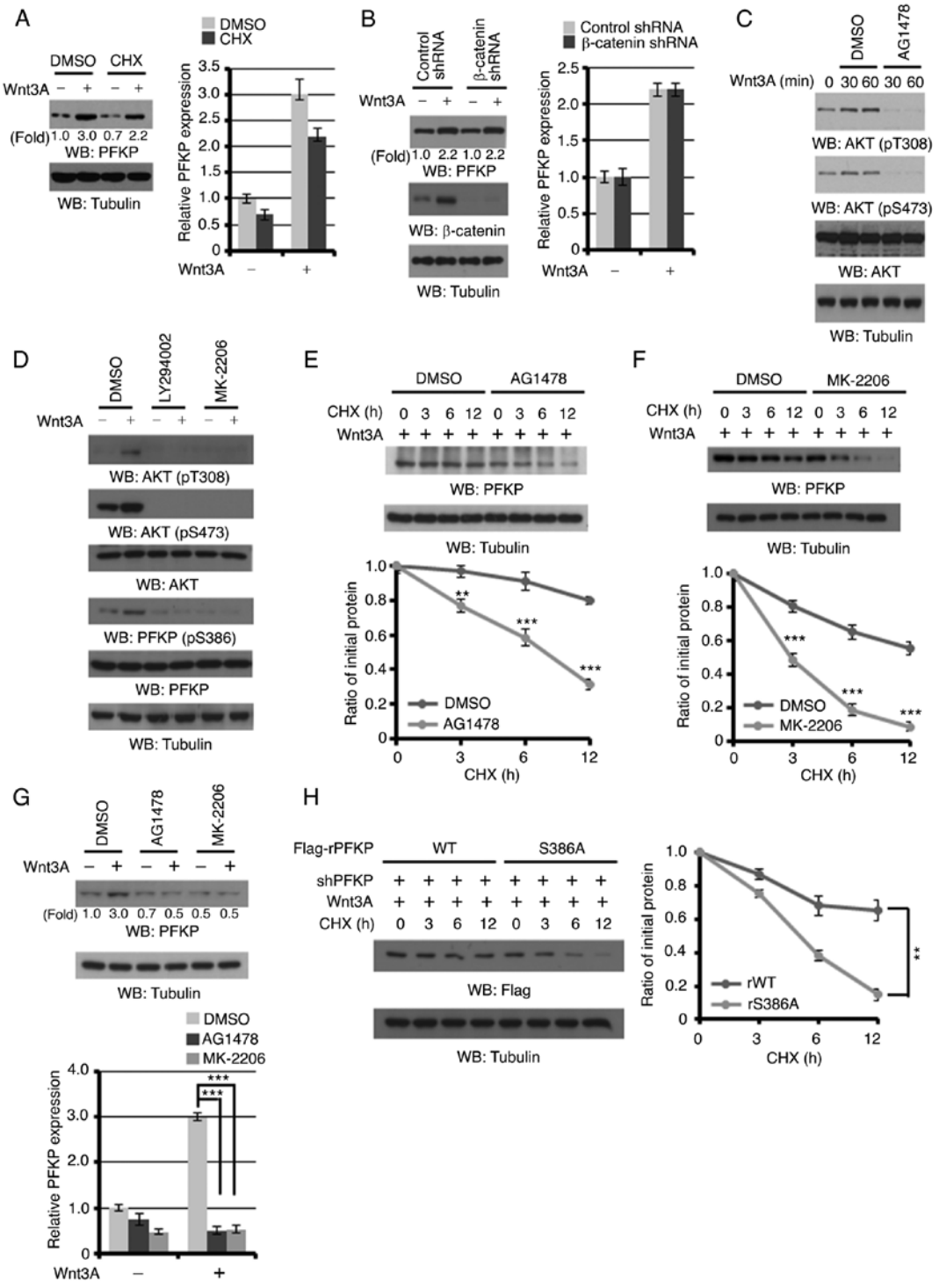

Figure 3. Role of PFKP S386 phosphorylation in the Wnt3A-induced PFKP expression. (A) Serum-starved A431 cells were pre-treated with or without CHX (100 μg/ml) for 1 h and stimulated subsequently with or without Wnt3A (20 ng/ml) for 12 h. Western blot analyses were performed with the indicated antibodies. Representative band intensity was quantified using ImageJ software. (B) Serum-starved A431 cells stably expressing β-catenin shRNA or a control shRNA were treated with or without Wnt3A (20 ng/ml) for 24 h. Western blot analyses were performed with the indicated antibodies. Representative band intensity was quantified using ImageJ software. (C) Serum-starved A431 cells were stimulated with or without Wnt3A (20 ng/ml) for the indicated periods of time in the presence of DMSO or AG1478 (1 μM). Western blot analyses were performed with the indicated antibodies. (D) Serum-starved A431 cells were pre-treated with DMSO, LY294002 (10 μM), or MK-2206 (5 μM) for 2 h and stimulated afterwards with Wnt3A (20 ng/ml) for 60 min. Western blot analyses were performed with the indicated antibodies. (E and F) Serum-starved A431 cells were pre-treated with Wnt3A (20 ng/ml) for 1 h and treated afterwards with CHX (100 μg/ml) for the indicated periods of time in the presence of DMSO, (E) AG1478 (1 μM), or (F) MK-2206 (5 μM). Western blot analyses were performed with the indicated antibodies (upper panel). The quantification of PFKP levels relative to tubulin is shown (bottom panel). The data represent the mean ± SD of three independent experiments. **P<0.01 and ***P<0.001 based on the Student's t-test. (G) Serum-starved A431 cells were pretreated with DMSO, AG1478 (1 μM), or MK-2206 (5 μM) for 2 h and stimulated afterwards with or without Wnt3A (20 ng/ml) for 24 h. Western blot analyses were performed with the indicated antibodies. Representative band intensity was quantified using ImageJ software. ***P<0.001 based on one-way ANOVA with Tukey's post hoc test. (H) A431 cells with or without the expression of PFKP shRNA and with or without the reconstituted expression of WT Flag-rPFKP or Flag-rPFKP S386A were pretreated with Wnt3A (20 ng/ml) for 1 h and subsequently treated with CHX (100 μg/ml) for the indicated periods of time. Western blot analyses were performed with the indicated antibodies (left panel). The quantification of PFKP levels relative to tubulin is shown (right panel). The data represent the mean ± SD of three independent experiments. **P<0.01 based on the Student's t-test. CHX, cycloheximide; PFKP, phosphofructokinase 1 platelet isoform.

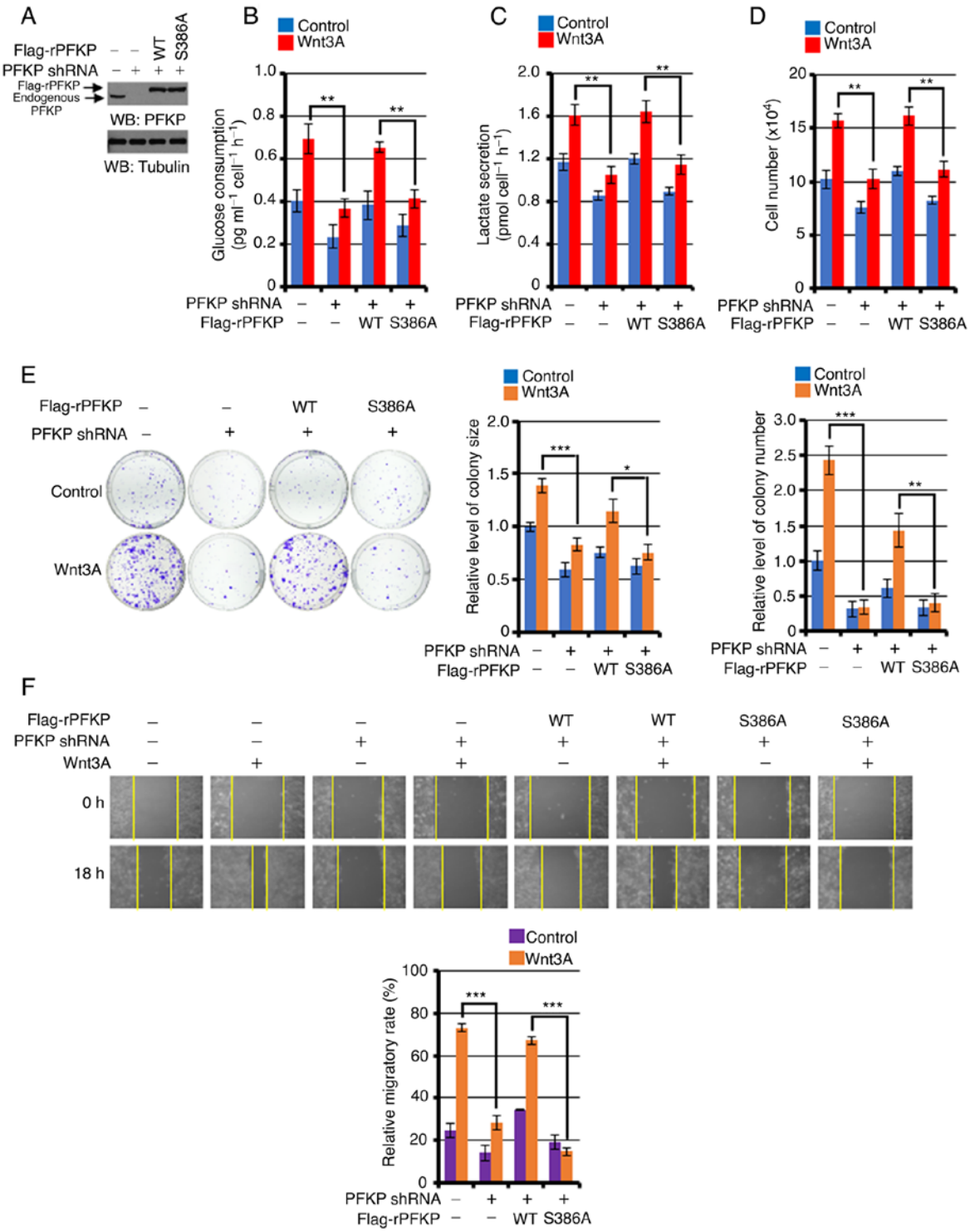

Figure 4. Role of PFKP S386 phosphorylation in the Wnt3A-induced the Warburg effect, and proliferation, colony formation and cancer cell migration. (A) PFKP expression was depleted and then reconstituted with WT Flag-rPFKP or Flag-rPFKP S386A in A431 cells. Western blot analyses were performed with the indicated antibodies. MG132 (10 μM) was added to the cells 6 h prior to harvesting to eliminate the potential effect of proteasomal degradation of PFKP. (B and C) A431 cells with or without the expression of PFKP shRNA and with or without the reconstituted expression of WT Flag-rPFKP or Flag-rPFKP S386A were cultured in serum-free DMEM with or without Wnt3A (20 ng/ml) for 48 h. The media were collected to analyze (B) glucose consumption and (C) lactate secretion. All results were normalized to the cell number. The data represent the mean ± SD of three independent experiments. **P<0.01 based on the Student's t-test. (D) A431 cells with or without the expression of PFKP shRNA and with or without the reconstituted expression of WT Flag-rPFKP or Flag-rPFKP S386A were cultured in 0.5% serum medium with or without Wnt3A (20 ng/ml) for 4 days and harvested for cell counting. The data represent the mean ± SD of three independent experiments. **P<0.01 based on the Student's t-test. (E) A431 cells with or without the expression of PFKP shRNA and with or without the reconstituted expression of WT Flag-rPFKP or Flag-rPFKP S386A were cultured in 10% serum medium with or without Wnt3A (20 ng/ml), for 12 days. The colonies were fixed with 10% formalin and stained with 0.1% crystal violet. Representative images are shown (left panel). Colony number (middle panel) and size (right panel) were analyzed. The data represent the mean ± SD of three independent experiments. *P<0.05, **P<0.01 and ***P<0.001 based on the Student's t-test. (F) Migratory ability of A431 cells with or without the expression of PFKP shRNA and with or without the reconstituted expression of WT Flag-rPFKP or Flag-rPFKP S386A was assessed by wound healing assay for 18 h with or without Wnt3A (20 ng/ml). Representative images are shown (upper panel). The quantification of migration ability is shown (bottom panel). The data represent the mean ± SD of three independent experiments. ***P<0.001 based on the Student's t-test. PFKP, phosphofructokinase 1 platelet isoform; WT, wild-type.

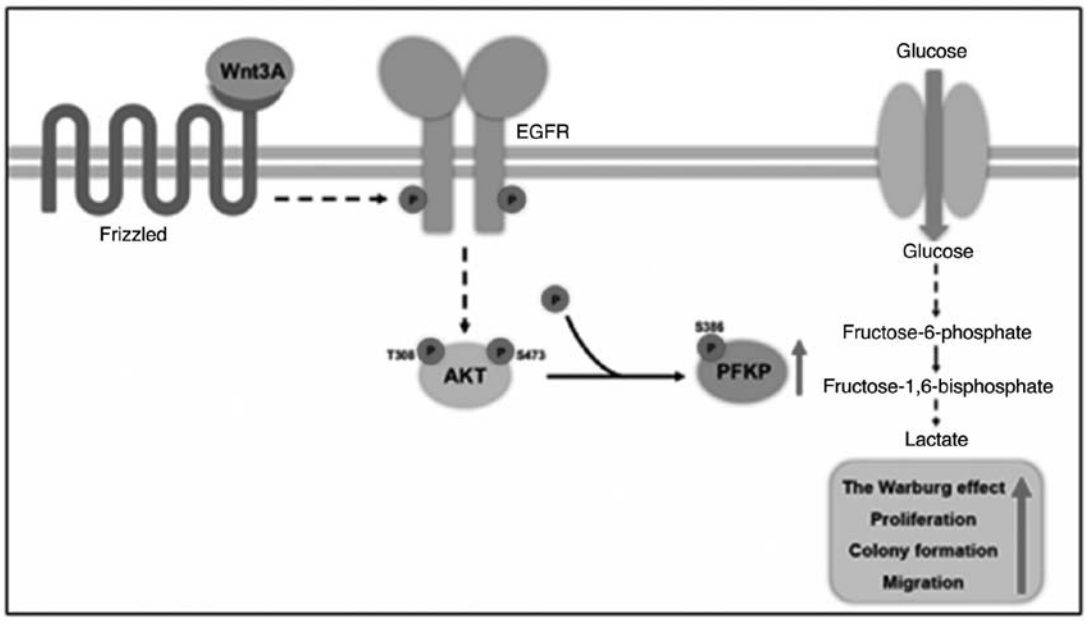

Figure 5. Schematic diagram of the proposed mechanism. Wnt3A stimulation resulted in EGFR transactivation in order to induce PI3K/AKT activation, which phosphorylated PFKP at S386 and stabilized PFKP protein, thereby promoting the Warburg effect, proliferation, colony formation and cancer cell migration.

production (Fig. 1E), proliferation (Fig. 1F), colony-forming ability (Fig. 1G) and migration (Fig. 1H) in the A431 cells. These results indicated that Wnt signaling successfully may transactivate EGFR in cancer cells, which is required for the Wnt-induced the Warburg effect, as well as proliferation, colony formation and cancer cell migration.

Wnt3A induces PFK enzyme activity and PFKP expression. PFK is critical for glycolysis (33), and its activity and expression is important for tumor development (37,39,40). Thus, the effect of Wnt signaling on PFK enzyme activity was examined in the present study. As shown in Fig. 2A, Wnt3A stimulation markedly induced PFK enzyme activity, which was significantly inhibited by treatment with AG1478 EGFR inhibitor, suggesting that Wnt signaling induced PFK activity through EGFR transactivation. Subsequently, the effect of Wnt signaling on PFK expression was determined. PFK includes PFK1 and PFK2 isoforms (33). Additionally, PFK1 includes PFKP, PFKM and PFKL isoforms. Furthermore, PFK2 [also known as 6-phosphofructo-2-kinase/fructose-2,6-bisphosphatase (PFKFB)], a bi-functional enzyme encoded by four different genes (*PFKFB1*, *PFKFB2*, *PFKFB3* and *PFKFB4*) with both a kinase and a phosphatase domain, is responsible for the production and degradation of fructose-2,6-bisphosphate (41). The aforementioned enzymes and their corresponding isoforms have been originally detected in different tissues: PFKFB1 in the liver and skeletal muscle, PFKFB2 in the heart tissue, PFKFB3 in the brain and PFKFB4 in the testis (42). The analyses of the isoform expression profiles using RT-qPCR and western blot analysis revealed that Wnt3A treatment did not markedly alter the PFK1 (Fig. 2B) and PFK2 (Fig. 2C) isoform mRNA expression levels and in A431 cells, whereas the PFKP protein expression levels, but not those of PFKL, PFKM and PFK2, were upregulated in the A431 cells (Fig. 2D), and the LN18, MDA-MB-231, SCC12 and SCC13 cells (Fig. S2) in response to Wnt3A stimulation. Consistent with these findings, immunofluorescence analyses with anti-PFKP antibody revealed that Wnt3A treatment enhanced PFKP expression in A431 cells (Fig. 2E). Taken together, it was observed that Wnt signaling increased PFK activity and PFKP expression. In order to determine the role of PFKP expression in Wnt-induced PFK activation, PFKP expression was depleted with the use of shRNA. It was then demonstrated that a reduction in PFKP expression significantly decreased the Wnt3A-induced total PFK enzyme activity in A431 cells (Fig. 2F), suggesting a crucial role of PFKP expression in Wnt signaling-induced PFK activation.

Wnt3A induces PFKP expression through EGFR/PI3K/AKT activation-induced PFKP S386 phosphorylation. The A431 cells were pre-treated with CHX to block protein synthesis, in order to determine whether PFKP protein expression is regulated by Wnt signaling. CHX treatment exerted a limited effect on Wnt3A-induced PFKP expression (Fig. 3A). These results suggest that Wnt signaling enhances PFKP expression primarily by enhancing PFKP stability. Of note, β-catenin depletion in A431 cells revealed that a reduction in β-catenin expression did not affect Wnt3A-induced PFKP protein expression (Fig. 3B), suggesting that Wnt signaling induces PFKP expression in the canonical Wnt-independent manner in cancer cells.

It has been previously reported by the authors that AKT phosphorylates PFKP at S386, which results in the inhibition of TRIM21 E3 ligase binding to PFKP and the subsequent TRIM21-mediated polyubiquitylation and degradation of PFKP, ultimately resulting in an increased PFKP expression (37). Wnt3A stimulation successfully induced AKT phosphorylation, which was blocked by treatment with AG1478 EGFR inhibitor (Fig. 3C). In addition, Wnt3A induced PFKP S386 phosphorylation in A431 cells (Fig. 3D; first and second lanes). As expected, treatment of the A431 cells with the

PI3K inhibitor, LY294002, or the AKT inhibitor, MK-2206, successfully blocked Wnt3A-induced AKT T308/S473 and PFKP S386 phosphorylation (Fig. 3D). Furthermore, the Wnt3A-induced half-life of endogenous PFKP (Fig. 3E and F) and PFKP expression (Fig. 3G) were markedly decreased following treatment with the AG1478 EGFR inhibitor or MK-2206 AKT inhibitor, respectively. In line with this finding, the Wnt3A-induced half-life of the PFKP S386A mutant was much shorter than that of its wild-type (WT) counterpart (Fig. 3H). These results indicated that EGFR/PI3K/AKT activation-induced PFKP S386 phosphorylation is required for Wnt-enhanced PFKP protein expression.

PFKP S386 phosphorylation is required for the Wnt3A-induced the Warburg effect, proliferation, colony formation and cancer cell migration. To investigate the role of PFKP S386 phosphorylation in the Wnt signaling-induced Warburg effect, cell proliferation, colony formation and migration, endogenous PFKP was depleted in A431 cells and the expression of RNAi-resistant (r) WT Flag-rPFKP or Flag-rPFKP S386A was reconstituted in these cells. The depletion of PFKP (Fig. 4A) markedly impaired Wnt3A-induced glucose consumption (Fig. 4B), lactate production (Fig. 4C), proliferation (Fig. 4D), colony formation ability (Fig. 4E) and cell migration (Fig. 4F); this inhibition was reversed by the expression of WT rPFKP, but not by the expression of rPFKP S386A mutant in A431 cells (Fig. 4A-F). Of note, Wnt3A stimulation or PFKP depletion did not affect LDHA enzyme expression and activity in A431 cells (Fig. S3). These results suggested that PFKP S386 phosphorylation may be important for the Wnt-induced the Warburg effect, as well as for proliferation, colony formation and cancer cell migration.

Discussion

Metabolic alterations have been observed in cancer cells, of which the Warburg effect is considered a common feature and critical for tumor development. Metabolic changes in cancer cells are regulated by microenvironmental and genetic factors. Wnt has been reported to be one of the environmental factors (10,11), and the abnormal activation of Wnt signaling has been observed in a number of human tumor types, which is considered important for tumor development (7-9). However, how Wnt signaling regulates metabolic alterations to promote tumor development remains unknown. In the present study, it was demonstrated that Wnt signaling directly regulated glycolysis through β-catenin signaling-independent PFKP upregulation. Mechanistically, Wnt3A signaling transactivated EGFR, leading to PI3K/AKT activation and culminating in increased PFKP stability through PFKP S386 phosphorylation. Wnt3A-induced PFKP S386 phosphorylation increased PFKP expression and PFK activity and promoted the Warburg effect, as well as proliferation, colony formation and cancer cell migration (Fig. 5). The current findings uncovered a novel mechanism, to the best of our knowledge, through which Wnt signaling directly regulates glycolysis in a PFKP S386 phosphorylation-dependent manner to promote tumor development.

EGFR overexpression has been detected in various human tumors, including epidermoid and breast carcinomas and GBM tumors and has been correlated with poor clinical prognosis (37,43,44). It has been reported that G protein-coupled receptors (GPCRs) stimulation could transactivate EGFR, in which metalloproteases (MMPs), such as a disintegrin and metalloproteases (ADAMs), matrix metalloproteinase-2 (MMP2) and matrix metalloproteinase-9 (MMP9), mediate EGFR ligand cleavage, leading to the activation of downstream signals (45-48). Frizzled family members have been functionalized as canonical GPCRs (49,50) that contain an N-terminal extra-cellular cysteine-rich domain to bind with glycoproteins of the Wnt family (51). Upon Wnt/Frizzled binding, diverse signaling pathways are activated through the phosphoprotein Dishevelled (22). Schlange *et al* (52) and Civenni *et al* (53) have reported that Wnt signaling induced the activation of EGFR through Dishevelled, Src, and the MMP-dependent release of soluble EGFR ligands, leading to the activation of ERK, inducing proliferation. Consistent with these reports, in the present study, Wnt3A stimulation induced the phosphorylation of EGFR in several cancer types. In addition, Wnt3A-induced EGFR phosphorylation was blocked by Src inhibition (data not shown). Since EGFR is amplified in most tumor cells, in addition to the canonical pathway Wnt signaling can activate more diverse signals, in order to promote tumor development through EGFR transactivation.

PFK1 is a rate-limiting enzyme in glycolysis (33). It has been reported both by the authors and others that PFKP is the prominent PFK1 isoform in GBM, ascites tumor cells, and breast carcinoma (37,54-56). In a previous study by the authors, it was revealed that PFKP was overexpressed in human GBM cell lines, primary GBM cells and GBM specimens (37). Furthermore, AKT activation enhanced the phosphorylation of PFKP at S386, resulting in the suppression of TRIM21 E3 ligase-mediated polyubiquitylation and the proteasomal degradation of PFKP. PFKP S386 phosphorylation enhanced PFKP expression and promoted aerobic glycolysis and brain tumor growth (37). In the present study, it was demonstrated that Wnt signaling induced PFKP S386 phosphorylation in an EGFR/PI3K/AKT activation-dependent manner, resulting in PFKP expression upregulation and PFK enzyme activity increase. PFKP S386 phosphorylation was important for the Wnt-induced Warburg effect, proliferation, colony formation and cancer cell migration.

In conclusion, the present study was demonstrated for the first time, to the best of our knowledge, that Wnt signaling directly regulated glycolysis-associated enzyme expression through the non-canonical Wnt pathway, in order to promote tumor development. The findings of the present study may provide insight, concerning the critical role of PFKP in fundamental biological processes for Wnt-induced tumor development.

Acknowledgements

LN18 and LN229 GBM cells were kindly provided by Dr Hyunggee Kim (Korea University, Seoul, Korea). U251 GBM cells were kindly provided by Dr Kyu Heo (Dongnam Institute of Radiological and Medical Sciences, Busan, Korea). The human epidermal squamous carcinoma cell lines, SCC12 and SCC13, were kindly provided by Dr Tae-Jin Yoon (Gyeongsang National University and Hospital, Jinju, Korea).

Funding

The present study was supported by the Dong-A University research fund.

Availability of data and materials

The datasets used and/or analyzed during the current study are available from the corresponding author on reasonable request.

Authors' contributions

SMJ, JSL, SHP and J-HL designed and performed experiments and analyzed data. SMJ and J-HL wrote the manuscript. SMJ, JSL, and SHP confirmed the authenticity of all the raw data. All authors have read and approved the final manuscript and agree to be accountable for all aspects of the research in ensuring that the accuracy or integrity of any part of the work are appropriately investigated and resolved.

Ethics approval and consent to participate

Not applicable.

Patient consent for publication

Not applicable.

Competing interests

The authors declare that they have no competing interests.

References

1. Acebron SP, Karaulanov E, Berger BS, Huang YL and Niehrs C: Mitotic wnt signaling promotes protein stabilization and regulates cell size. Mol Cell 54: 663-674, 2014.
2. Atlasi Y, Noori R, Gaspar C, Franken P, Sacchetti A, Rafati H, Mahmoudi T, Decraene C, Calin GA, Merrill BJ and Fodde R: Wnt signaling regulates the lineage differentiation potential of mouse embryonic stem cells through Tcf3 down-regulation. PLoS Genet 9: e1003424, 2013.
3. Esen E, Chen J, Karner CM, Okunade AL, Patterson BW and Long F: WNT-LRP5 signaling induces Warburg effect through mTORC2 activation during osteoblast differentiation. Cell Metab 17: 745-755, 2013.
4. Clevers H: Wnt/beta-catenin signaling in development and disease. Cell 127: 469-480, 2006.
5. Angers S and Moon RT: Proximal events in Wnt signal transduction. Nat Rev Mol Cell Biol 10: 468-477, 2009.
6. Clevers H, Loh KM and Nusse R: Stem cell signaling. An integral program for tissue renewal and regeneration: Wnt signaling and stem cell control. Science 346: 1248012, 2014.
7. Anastas JN and Moon RT: WNT signalling pathways as therapeutic targets in cancer. Nat Rev Cancer 13: 11-26, 2013.
8. Lang CMR, Chan CK, Veltri A and Lien WH: Wnt signaling pathways in keratinocyte carcinomas. Cancers (Basel) 11: 1216, 2019.
9. Lee Y, Lee JK, Ahn SH, Lee J and Nam DH: WNT signaling in glioblastoma and therapeutic opportunities. Lab Invest 96: 137-150, 2016.
10. Milovanovic T, Planutis K, Nguyen A, Marsh JL, Lin F, Hope C and Holcombe RF: Expression of Wnt genes and frizzled 1 and 2 receptors in normal breast epithelium and infiltrating breast carcinoma. Int J Oncol 25: 1337-1342, 2004.
11. Benhaj K, Akcali KC and Ozturk M: Redundant expression of canonical Wnt ligands in human breast cancer cell lines. Oncol Rep 15: 701-707, 2006.
12. Zheng W, Yao M, Fang M, Pan L, Wang L, Yang J, Dong Z and Yao D: Oncogenic Wnt3a: A candidate specific marker and novel molecular target for hepatocellular carcinoma. J Cancer 10: 5862-5873, 2019.
13. Kaur N, Chettiar S, Rathod S, Rath P, Muzumdar D, Shaikh ML and Shiras A: Wnt3a mediated activation of Wnt/β-catenin signaling promotes tumor progression in glioblastoma. Mol Cell Neurosci 54: 44-57, 2013.
14. Jing Q, Li G, Chen X, Liu C, Lu S, Zheng H, Ma H, Qin Y, Zhang D, Zhang S, *et al*: Wnt3a promotes radioresistance via autophagy in squamous cell carcinoma of the head and neck. J Cell Mol Med 23: 4711-4722, 2019.
15. He S, Lu Y, Liu X, Huang X, Keller ET, Qian CN and Zhang J: Wnt3a: Functions and implications in cancer. Chin J Cancer 34: 554-562, 2015.
16. Verras M, Brown J, Li X, Nusse R and Sun Z: Wnt3a growth factor induces androgen receptor-mediated transcription and enhances cell growth in human prostate cancer cells. Cancer Res 64: 8860-8866, 2004.
17. Grumolato L, Liu G, Mong P, Mudbhary R, Biswas R, Arroyave R, Vijayakumar S, Economides AN and Aaronson SA: Canonical and noncanonical Wnts use a common mechanism to activate completely unrelated coreceptors. Genes Dev 24: 2517-2530, 2010.
18. Katoh M: Canonical and non-canonical WNT signaling in cancer stem cells and their niches: Cellular heterogeneity, omics reprogramming, targeted therapy and tumor plasticity (Review). Int J Oncol 51: 1357-1369, 2017.
19. Klaus A and Birchmeier W: Wnt signalling and its impact on development and cancer. Nat Rev Cancer 8: 387-398, 2008.
20. Polakis P: The many ways of Wnt in cancer. Curr Opin Genet Dev 17: 45-51, 2007.
21. Reya T and Clevers H: Wnt signalling in stem cells and cancer. Nature 434: 843-850, 2005.
22. Duchartre Y, Kim YM and Kahn M: The Wnt signaling pathway in cancer. Crit Rev Oncol Hematol 99: 141-149, 2016.
23. Polakis P: Wnt signaling and cancer. Genes Dev 14: 1837-1851, 2000.
24. Corda G and Sala A: Non-canonical WNT/PCP signalling in cancer: Fzd6 takes centre stage. Oncogenesis 6: e364, 2017.
25. Kurayoshi M, Oue N, Yamamoto H, Kishida M, Inoue A, Asahara T, Yasui W and Kikuchi A: Expression of Wnt-5a is correlated with aggressiveness of gastric cancer by stimulating cell migration and invasion. Cancer Res 66: 10439-10448, 2006.
26. Weeraratna AT, Jiang Y, Hostetter G, Rosenblatt K, Duray P, Bittner M and Trent JM: Wnt5a signaling directly affects cell motility and invasion of metastatic melanoma. Cancer Cell 1: 279-288, 2002.
27. Vander Heiden MG, Cantley LC and Thompson CB: Understanding the Warburg effect: The metabolic requirements of cell proliferation. Science 324: 1029-1033, 2009.
28. Warburg O: On the origin of cancer cells. Science 123: 309-314, 1956.
29. Cairns RA, Harris IS and Mak TW: Regulation of cancer cell metabolism. Nat Rev Cancer 11: 85-95, 2011.
30. Hsu PP and Sabatini DM: Cancer cell metabolism: Warburg and beyond. Cell 134: 703-707, 2008.
31. Pate KT, Stringari C, Sprowl-Tanio S, Wang K, TeSlaa T, Hoverter NP, McQuade MM, Garner C, Digman MA, Teitell MA, *et al*: Wnt signaling directs a metabolic program of glycolysis and angiogenesis in colon cancer. EMBO J 33: 1454-1473, 2014.
32. Lee SY, Jeon HM, Ju MK, Kim CH, Yoon G, Han SI, Park HG and Kang HS: Wnt/Snail signaling regulates cytochrome C oxidase and glucose metabolism. Cancer Res 72: 3607-3617, 2012.
33. Mor I, Cheung EC and Vousden KH: Control of glycolysis through regulation of PFK1: Old friends and recent additions. Cold Spring Harb Symp Quant Biol 76: 211-216, 2011.
34. Moreno-Sanchez R, Rodriguez-Enriquez S, Marin-Hernandez A and Saavedra E: Energy metabolism in tumor cells. FEBS J 274: 1393-1418, 2007.
35. Dunaway GA and Kasten TP: Nature of the subunits of the 6-phosphofructo-1-kinase isoenzymes from rat tissues. Biochem J 242: 667-671, 1987.
36. Kahn A, Meienhofer MC, Cottreau D, Lagrange JL and Dreyfus JC: Phosphofructokinase (PFK) isozymes in man. I. Studies of adult human tissues. Hum Genet 48: 93-108, 1979.
37. Lee JH, Liu R, Li J, Zhang C, Wang Y, Cai Q, Qian X, Xia Y, Zheng Y, Piao Y, *et al*: Stabilization of phosphofructokinase 1 platelet isoform by AKT promotes tumorigenesis. Nat Commun 8: 949, 2017.

38. Livak KJ and Schmittgen TD: Analysis of relative gene expression data using real-time quantitative PCR and the 2(-Delta Delta C(T)) method. Methods 25: 402-408, 2001.
39. Lee JH, Liu R, Li J, Wang Y, Tan L, Li XJ, Qian X, Zhang C, Xia Y, Xu D, *et al*: EGFR-Phosphorylated platelet isoform of phosphofructokinase 1 promotes PI3K activation. Mol Cell 70: 197-210.e7, 2018.
40. Lee JH, Shao F, Ling J, Lu S, Liu R, Du L, Chung JW, Koh SS, Leem SH, Shao J, *et al*: Phosphofructokinase 1 platelet isoform promotes β-catenin transactivation for tumor development. Front Oncol 10: 211, 2020.
41. Stine ZE and Dang CV: Stress eating and tuning out: Cancer cells re-wire metabolism to counter stress. Crit Rev Biochem Mol Biol 48: 609-619, 2013.
42. Rider MH, Bertrand L, Vertommen D, Michels PA, Rousseau GG and Hue L: 6-phosphofructo-2-kinase/fructose-2,6-bisphosphatase: Head-to-head with a bifunctional enzyme that controls glycolysis. Biochem J 381(Pt 3): 561-579, 2004.
43. Cancer Genome Atlas Research Network: Comprehensive genomic characterization defines human glioblastoma genes and core pathways. Nature 455: 1061-1068, 2008.
44. Avraham R and Yarden Y: Feedback regulation of EGFR signalling: Decision making by early and delayed loops. Nat Rev Mol Cell Biol 12: 104-117, 2011.
45. Prenzel N, Zwick E, Daub H, Leserer M, Abraham R, Wallasch C and Ullrich A: EGF receptor transactivation by G-protein-coupled receptors requires metalloproteinase cleavage of proHB-EGF. Nature 402: 884-888, 1999.
46. Blobel CP: ADAMs: Key components in EGFR signalling and development. Nat Rev Mol Cell Biol 6: 32-43, 2005.
47. Ohtsu H, Dempsey PJ and Eguchi S: ADAMs as mediators of EGF receptor transactivation by G protein-coupled receptors. Am J Physiol Cell Physiol 291: C1-C10, 2006.
48. Roelle S, Grosse R, Aigner A, Krell HW, Czubayko F and Gudermann T: Matrix metalloproteinases 2 and 9 mediate epidermal growth factor receptor transactivation by gonadotropin-releasing hormone. J Biol Chem 278: 47307-47318, 2003.
49. Koval A and Katanaev VL: Wnt3a stimulation elicits G-protein-coupled receptor properties of mammalian Frizzled proteins. Biochem J 433: 435-440, 2011.
50. Nichols AS, Floyd DH, Bruinsma SP, Narzinski K and Baranski TJ: Frizzled receptors signal through G proteins. Cell Signal 25: 1468-1475, 2013.
51. Yang-Snyder J, Miller JR, Brown JD, Lai CJ and Moon RT: A frizzled homolog functions in a vertebrate Wnt signaling pathway. Curr Biol 6: 1302-1306, 1996.
52. Schlange T, Matsuda Y, Lienhard S, Huber A and Hynes NE: Autocrine WNT signaling contributes to breast cancer cell proliferation via the canonical WNT pathway and EGFR transactivation. Breast Cancer Res 9: R63, 2007.
53. Civenni G, Holbro T and Hynes NE: Wnt1 and Wnt5a induce cyclin D1 expression through ErbB1 transactivation in HC11 mammary epithelial cells. EMBO Rep 4: 166-171, 2003.
54. Sanchez-Martinez C and Aragon JJ: Analysis of phosphofructokinase subunits and isozymes in ascites tumor cells and its original tissue, murine mammary gland. FEBS Lett 409: 86-90, 1997.
55. Moon JS, Kim HE, Koh E, Park SH, Jin WJ, Park BW, Park SW and Kim KS: Kruppel-like factor 4 (KLF4) activates the transcription of the gene for the platelet isoform of phosphofructokinase (PFKP) in breast cancer. J Biol Chem 286: 23808-23816, 2011.
56. Wang G, Xu Z, Wang C, Yao F, Li J, Chen C and Sun S: Differential phosphofructokinase-1 isoenzyme patterns associated with glycolytic efficiency in human breast cancer and paracancer tissues. Oncol Lett 6: 1701-1706, 2013.